Journal of Materials Chemistry C

ROYAL SOCIETY OF CHEMISTRY

COMMUNICATION

View Article Online
View Journal | View Issue

Cite this: J. Mater. Chem. C, 2024, 12, 8296

Received 3rd April 2024,
Accepted 16th May 2024

DOI: 10.1039/d4tc01355g

rsc.li/materials-c

Designing an aromatic moiety-free neutral luminescent manganese(II) halide scintillator for efficient X-ray imaging†

Xiaokang Zheng,[abd] Zijian Zhou,[c] Zikang Li,[ab] Ka-Yan Tran,[ab] Pengfei She,[ab] Hua Wang,[d] Wai-Yeung Wong,*[ab] Qiang Zhao*[c] and Peng Tao*[ab]

An aromatic moiety-free strategy is proposed for the effective excited state manipulation of the neutral luminescent manganese(II) halide. Interestingly, compared to the traditional monodentate ligand-based manganese(II) complexes, a dramatic enhancement of photoluminescent quantum yield of 0.413 is achieved by incorporating tri(pyrrolidin-1-yl)phosphine oxide (TPPO) as a new ligand without any aromatic moiety into the manganese(II) complex. The designed aromatic moiety-free neutral luminescent manganese(II) bromide ($TPPOMnBr_2$) featuring an intense green emission (512 nm) and a short emission lifetime (0.564 ms) is employed to realize efficient X-ray imaging with a high spatial resolution value of 11.3 lp mm^{-1} and a low detection limit of 34.95 nGy s^{-1}, making it a promising candidate for high-performance X-ray detection in the future.

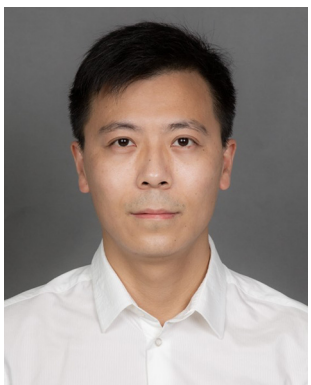

Peng Tao

Dr Peng Tao obtained his BSc and PhD degrees from Taiyuan University of Technology, with the PhD study supervised by Prof. Wei Huang, an academician of the Chinese Academy of Sciences. From 2012 to 2018, he joined as a visiting student at State Key Laboratory of Organic Electronics and Information Displays, Nanjing University of Posts and Telecommunications under the supervision of Prof. Qiang Zhao. After postdoctoral work with Prof. Wai-Yeung Wong at The Hong Kong Polytechnic University (PolyU), he was appointed as a Research Assistant Professor at PolyU from Jul 2020. His current research interest focuses on the design and synthesis of advanced functional molecules and polymers including luminescent transition-metal complexes and π-conjugated compounds for multifunctional applications.

X-ray scintillators converting high-energy X-ray radiation into ultraviolet or visible light have received great interest for their potential application in various fields ranging from healthcare to security.[1–3] In the past few decades, many types of materials have been discovered for X-ray scintillators.[4–6] Currently, inorganic materials (*e.g.*, Tl-doped CsI/NaI, $CaWO_4$, $Bi_4Ge_3O_{12}$, $(Lu,Y)_2SiO_5$, $YTaO_4$, $Lu_3Al_5O_{12}$:Ce, *etc.*) represent an important class of commercial X-ray scintillators.[4–7] These inorganic scintillators usually show strong radioluminescence (RL) and high X-ray attenuation efficiency. However, they still have some limitations in applications. For instance, the Tl-doped CsI/NaI scintillators are sensitive to humidity. The preparation of the ceramic-type scintillators needs very high temperature (above 800 °C). The inorganic scintillators may not be suitable for the fabrication of flexible devices due to the inherent brittleness of the crystal, and they also cannot be processed by solution methods.[4–7] Recently, lead-based perovskite-type emitters have emerged as a new class of X-ray scintillators, which show highly efficient photoluminescence quantum yield (PLQY), excellent solution processability, inherent flexibility, *etc.*[8] The lead-based perovskite scintillators usually suffer from poor stability and toxicity.[8] Thus, it is necessary to further develop new

[a] Department of Applied Biology and Chemical Technology and Research Institute for Smart Energy, The Hong Kong Polytechnic University, Hung Hom, Hong Kong, China
[b] The Hong Kong Polytechnic University Shenzhen Research Institute, Shenzhen 518057, China. E-mail: wai-yeung.wong@polyu.edu.hk, pengtao@polyu.edu.hk
[c] State Key Laboratory of Organic Electronics and Information Displays, Institute of Advanced Materials (IAM) & Institute of Flexible Electronics (Future Technology), Nanjing University of Posts and Telecommunications, Nanjing 210023, China. E-mail: iamqzhao@njupt.edu.cn
[d] MOE Key Laboratory of Interface Science and Engineering in Advanced Materials, Taiyuan University of Technology, Taiyuan 030024, China

† Electronic supplementary information (ESI) available: Synthesis, characterization, CCDC deposition number and other data. CCDC 2336965. For ESI and crystallographic data in CIF or other electronic format see DOI: https://doi.org/10.1039/d4tc01355g

high-performance scintillators with stable structure, excellent solution processability, and low toxicity for practical application.

As a cheap transition-metal complex, manganese(II) emitters have drawn increasing attention owing to their appealing photophysical properties, flexible structural design, and eco-friendly nature, showing great potential for X-ray scintillators.[7,9,10] In general, the luminescent manganese(II) complexes can be divided into ionic and neutral ones.[9,10] The hydrophobic nature of the neutral complexes makes them good candidates for stable X-ray scintillators. However, the luminescent efficiency of the neutral manganese(II) complexes is far behind that of the ionic ones, especially for the manganese(II) complexes based on the monodentate ligands, hindering their application in high-performance X-ray imaging.[9a,11–14] For example, most of the reported monodentate ligand-based manganese(II) complexes exhibit very low PLQYs or are non-emissive at room temperature.[9a,11–14] Therefore, from the perspective of molecular design, how to effectively tune the excited states (*e.g.*, enhancement of the PLQY, *etc.*) of this class of manganese(II) complexes will be the research focus.

In this communication, we propose an aromatic moiety-free strategy for the effective manipulation of the excited state of the neutral manganese(II) complex (**TPPOMnBr$_2$**). We selected tri(pyrrolidin-1-yl)phosphine oxide (TPPO) as the new monodentate ligand, which does not contain any aromatic moiety. The TPPO ligand featuring a twisted cycloalkane structure with multiple C–H bonds can provide steric hindrance and enhance the distance among the complex molecules, potentially suppressing the excitation energy migration among manganese(II) centres. The prepared complex exhibits both intense photoluminescence (PL) under UV light and radioluminescence under X-ray radiation in the crystal state. Notably, compared to the traditional monodentate ligand-based manganese(II) complexes, a remarkable enhancement of the PLQY of 0.413 is realized for the manganese(II) complex. The designed aromatic moiety-free neutral complex **TPPOMnBr$_2$** showing a bright green emission and a short emission lifetime was also used to demonstrate efficient X-ray imaging with a high spatial resolution value of 11.3 lp mm^{-1} and a low detection limit of 34.95 nGy s^{-1}, indicating its great potential for high-performance X-ray detection.

The target complex **TPPOMnBr$_2$** was prepared by stirring $MnBr_2{\cdot}4H_2O$ and free ligand tri(pyrrolidin-1-yl)phosphine oxide in a stoichiometric ratio in the mixed solvents of CH_2Cl_2 and ethanol at 25 °C for 12 h under air (Scheme S1, ESI†). The complex **TPPOMnBr$_2$** can be crystallized as light green, bulk crystals with a large size in the centimetre range by slowly evaporating the mixed solvents of CH_2Cl_2 and ethanol at room temperature. The crystals show excellent stability to the air and moisture under ambient conditions. A photograph of the **TPPOMnBr$_2$** crystal under room light is shown in Fig. 1a. The structure of **TPPOMnBr$_2$** in the crystal state was confirmed by single crystal X-ray diffraction (XRD) at room temperature (Fig. 1b). The complex crystallizes in the monoclinic $P2_1/c$ space group and possesses a zero-dimensional structure at the molecular level (Table S1, ESI†). From the crystal structure in Fig. 1b, similar to the reported manganese(II) complexes,[9]

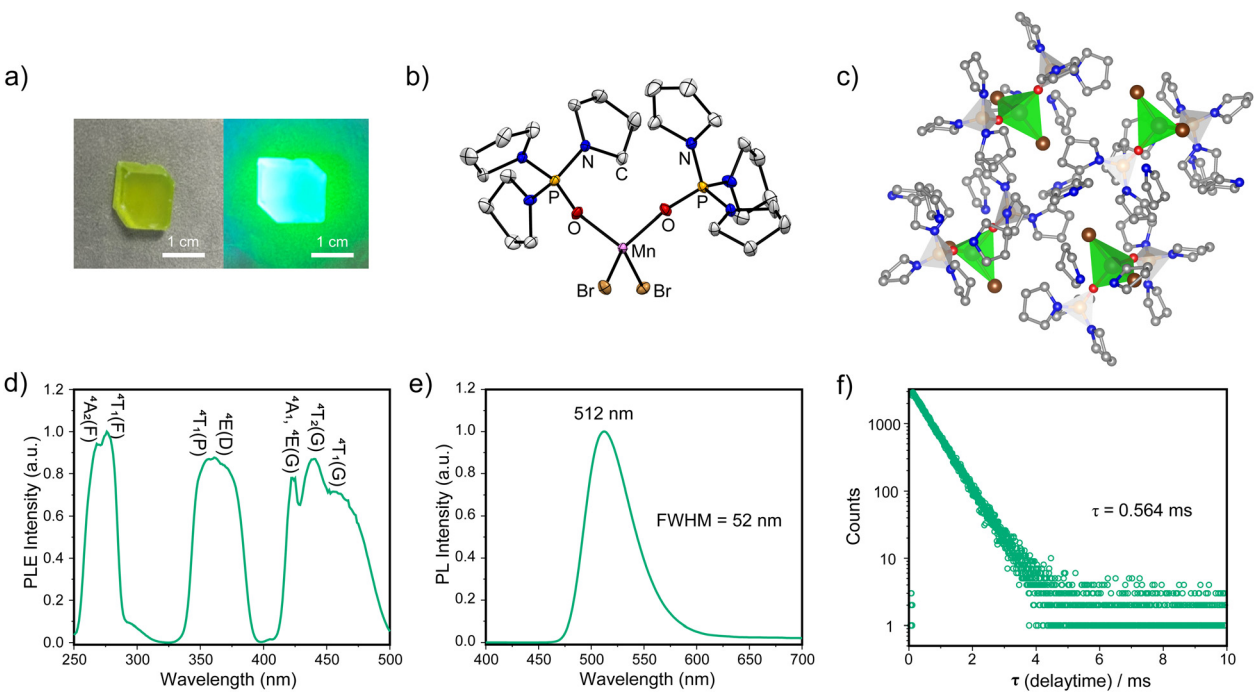

Fig. 1 (a) The photograph of the **TPPOMnBr$_2$** crystal under room light (left) and UV light of 365 nm (right). (b) The crystal structure and (c) molecular packing of **TPPOMnBr$_2$** (CCDC 2336965†, the hydrogen atoms omitted for clarity) at room temperature. (d) The PLE spectrum monitored at 512 nm, (e) the PL spectrum (λ_{ex} = 277 nm), and (f) the luminescent decay curve (λ_{ex} = 277 nm) of **TPPOMnBr$_2$** in the crystal state at room temperature.

the manganese(II) ion adopts a slightly distorted tetrahedral configuration (bond angles of 104.52° for O–Mn–O, and 115.50° for Br–Mn–Br), and coordinates to two bromide ions and two oxygen atoms from the phosphine oxide ligands. The bond lengths are 2.479 and 2.495 Å for the Mn–Br bonds, and 2.008 and 2.019 Å for the Mn–O bonds, respectively (Table S2, ESI†), which are also consistent with the reported analogues.[9,10] Moreover, no solvent molecule was embedded in the crystal, indicating that the molecules of the complex can tightly pack with each other *via* van der Waals interactions (*e.g.*, the weak interactions between the Br atom and H atom of the carbon–hydrogen bond) to form a stable crystal at room temperature (Fig. 1c and Fig. S2, ESI†). The shortest distance between the adjacent metal centre of the complex is 9.173 Å in the crystals, which could effectively suppress the excitation energy migration among manganese(II) centres to avoid PL quenching.[7] The experimental powder XRD pattern well agreed with the simulated one, implying the pure phase of the obtained crystals (Fig. S1, ESI†).

Under the excitation of UV light, the crystals of the complex emit a bright green luminescence peaking at 512 nm with a narrow full width at half maximum (FWHM) of 52 nm and 1931 Commission Internationale de l'Elcairage (CIE) coordinates of (0.20, 0.63) (Fig. 1a and e and Table S3, ESI†), which is attributed to the characteristic $^4T_1(G) \rightarrow {}^6A_1$ radiative electronic transition of the manganese(II) centre.[10] Notably, the PLQY of **TPPOMnBr$_2$** is remarkably enhanced to 0.413 in the crystal state at room temperature (Fig. S3c, ESI†), which is much higher than that of most reported monodentate ligand-based manganese(II) analogues (*e.g.*, triphenylphosphine oxide-based ones, *etc.*),[9a,11–14] indicating the effective manipulation of the excited state by the incorporated tri(pyrrolidin-1-yl)phosphine oxide ligands. The emission spectrum of the complex after 2 months in a wet environment is the same as that of the fresh sample (Fig. S3a, ESI†), implying the high stability to the moisture. The excitation and emission map for photoluminescence from the complex shows three bands consistent with its excitation spectrum. No obvious shift in emission can be observed with the change of excitation, implying the direct d–d transition in the manganese(II) centre (Fig. S3b, ESI†). The increased PLQY may be attributed to the high triplet energy level of the aromatic moiety-free ligand and the tight molecular packing in the crystals, suppressing the nonradiative deactivation process. The photoluminescence excitation (PLE) spectrum monitored at 512 nm for the complex shows multiple bands (Fig. 1d), and the three bands from the low energy band to high energy band could be attributed to the electronic transitions of $^6A_1 \rightarrow {}^4T_1(G)/{}^4T_2(G)/{}^4A_1(G)/{}^4E(G)$, $^6A_1 \rightarrow {}^4E(D)/{}^4T_1(P)$, and $^6A_1 \rightarrow {}^4T_1(F)/{}^4A_2(F)$ in the tetrahedral manganese(II) centre.[9a] From Fig. 1f, the luminescent lifetime for **TPPOMnBr$_2$** was determined to be 0.564 ms (single index), which is similar to the timescale of the lifetime for the typical manganese(II) bromides.[9a]

In order to have a deeper insight into the electronic structure of the designed complex, the energy-band structure in the crystal state was further calculated based on the crystal data by using the Cambridge sequential total energy package (CASTEP). Fig. 2a shows the calculated band structure of **TPPOMnBr$_2$**. The flat band edges of the valence band maximum (VBM) and conduction band minimum (CBM) of **TPPOMnBr$_2$** were observed, suggesting negligible wavefunction overlap and electronic coupling.[15] The VBM and CBM were composed of Mn 3d and Br 2p atomic orbitals according to the calculated projected density of states (PDOS) (Fig. 2b). In addition, as shown in Fig. 2c and d, the charge density distributions of the CBM were mainly located in the vacancy of the **TPPOMnBr$_2$** tetrahedral centre, and only a little CBM was localized in the ligands, implying that the ligands participated in the emission of the complex in a small amount. The VBM was contributed by the **TPPOMnBr$_2$** tetrahedral centre, with no obvious charge density overlap between the $MnBr_2O_2$ unit, indicating that the individual $MnBr_2O_2$ unit was the emission centre, and exhibited a strong quantum confinement effect.[16]

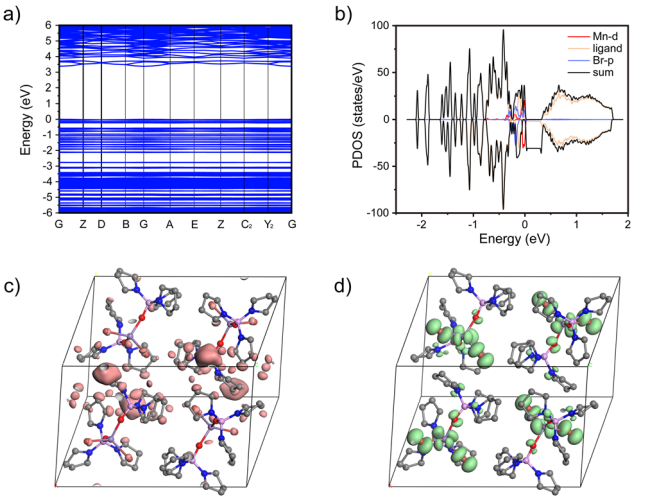

Fig. 2 (a) Calculated energy-band structure and (b) PDOS of **TPPOMnBr$_2$** in the crystal state. Partial charge density plots for the CBM (c) and VBM (d) (the hydrogen atoms are omitted for clarity).

The high PLQY of **TPPOMnBr$_2$** makes it a promising candidate for use as an X-ray scintillator. The X-ray absorption and radioluminescence properties of **TPPOMnBr$_2$** were further investigated. The absorbance of high-energy X-ray photons (1 MeV to 10^3 MeV) of **TPPOMnBr$_2$** shows almost the same order of magnitude values as that of the commercial scintillator $Lu_3Al_5O_{12}$:Ce (LuAG:Ce) (Fig. 3a). The X-ray attenuation efficiency of **TPPOMnBr$_2$** with different X-ray photon energies and thicknesses was also measured, which exhibited 80% X-ray attenuation efficiency at the thicknesses of 0.4 mm (Fig. 3b and c). Under the excitation of X-ray radiation, complex **TPPOMnBr$_2$** emits an intense green radioluminescence, which is the same as the PL spectrum under UV light (Fig. S4, ESI†). The intensity of the radioluminescence enhances linearly with the increase in the X-ray dose rate (Fig. S5 and S6, ESI†). As shown in Fig. 3e, the limit of detection was determined to be 34.95 nGy s^{-1} for **TPPOMnBr$_2$** (signal-to-noise ratio at 3), indicating the low limit of detection of the designed complex. **TPPOMnBr$_2$** exhibits a high relative light yield of

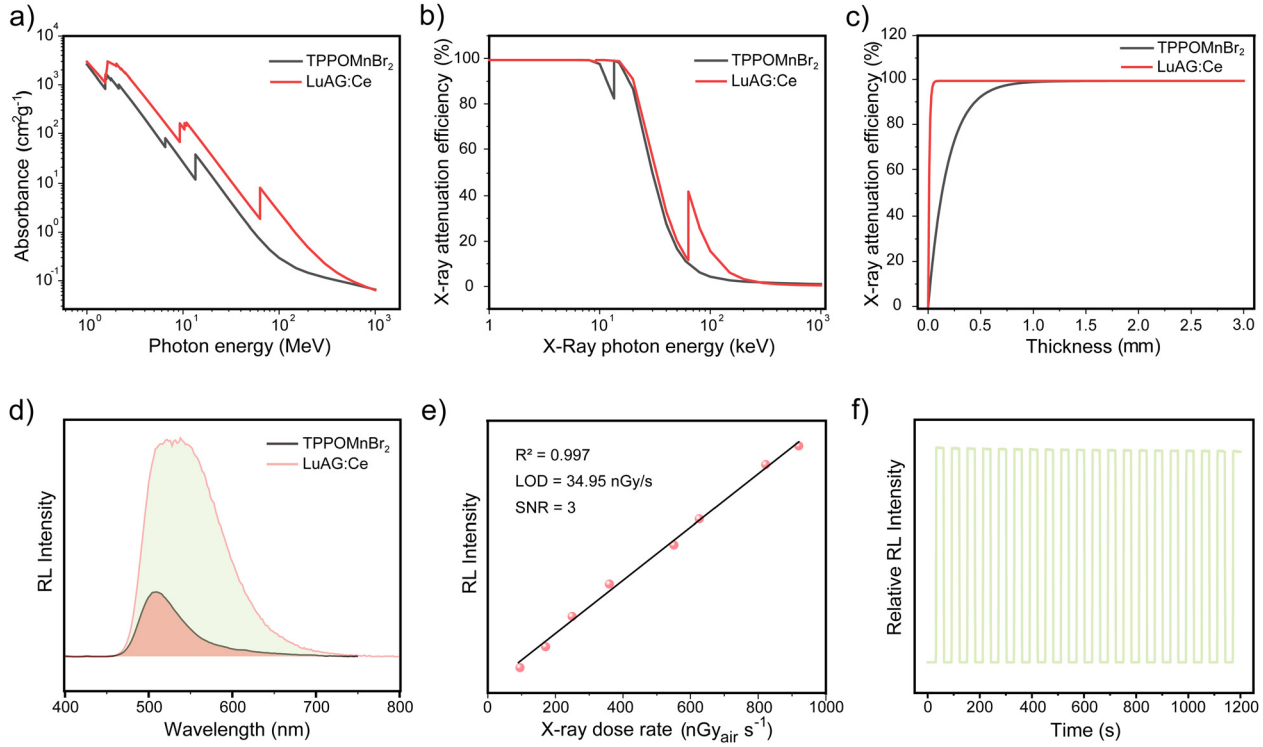

Fig. 3 (a) X-ray absorbance of high-energy photons of **TPPOMnBr$_2$** and LuAG:Ce. X-ray attenuation efficiencies of **TPPOMnBr$_2$** and LuAG:Ce with different X-ray photon energies (b) and thicknesses (c). (d) The RL intensity of the **TPPOMnBr$_2$** crystal and LuAG:Ce. (e) Linear dependence between the RL intensity of the **TPPOMnBr$_2$** crystal and X-ray dose rate with the lowest detection limit (LOD) confirmed at the signal-noise ratio (SNR) of 3. (f) X-ray irradiation stability of the **TPPOMnBr$_2$** crystal upon X-ray irradiation for 20 cycles. X-ray irradiation was switched on for 30 s and then switched off for 20 s in each cycle. Note: The photon energy range of the X-ray light involved in testing is from 5 keV to 30 keV.

10567 photons MeV^{-1} by using LuAG:Ce (22000 photons MeV^{-1}) as the reference,[9c] demonstrating the high efficiency of radioluminescence (Fig. 4d). The stability of **TPPOMnBr$_2$** to the X-ray irradiation was also evaluated by monitoring the RL intensity change upon X-ray irradiation for 20 cycles (Fig. 3f). The RL intensity of **TPPOMnBr$_2$** only decreased by 1.6% after 20 cycles of X-ray irradiation, indicating the excellent stability to X-ray irradiation.

Considering the excellent radioluminescence properties of **TPPOMnBr$_2$**, the X-ray imaging performances were further investigated by doping **TPPOMnBr$_2$** into poly(methyl methacrylate) (PMMA) with a weight ratio of 1 : 1. The film containing **TPPOMnBr$_2$** was prepared by a drop-coating method. The prepared film scintillator also showed intense green radioluminescence originated from the **TPPOMnBr$_2$** emitter. The PLQY of the **TPPOMnBr$_2$**-doped PMMA film was determined to be 0.148 (Fig. S3d, ESI†), which is lower than that in the crystal state. To estimate the spatial resolution of the **TPPOMnBr$_2$**-based film scintillator, by using X-ray imaging of the standard resolution test pattern plate, clear alternately shaded stripes could be observed around the spatial resolution value of 10.5 lp mm^{-1} (Fig. 4a). The spatial resolution of the film scintillator was also evaluated by the modulation transfer function (MTF) calculation from the standard X-ray slant edge test.[9c] At an MTF value of 0.2, the spatial resolution of the film scintillator was determined to be up to 11.3 lp mm^{-1} (Fig. 4d),

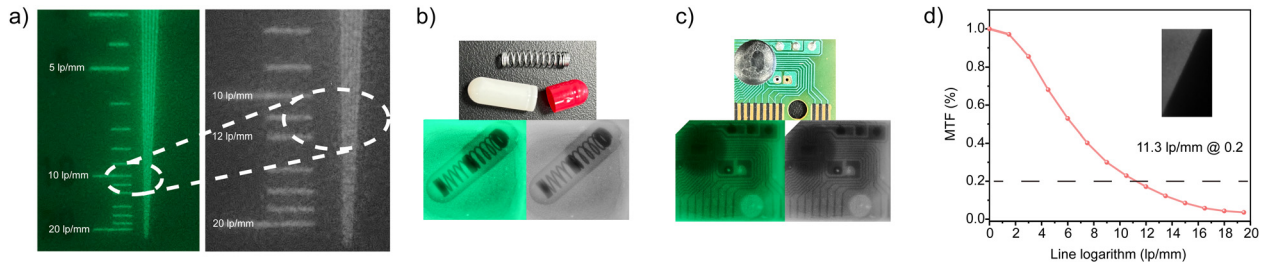

Fig. 4 (a) The spatial resolution of X-ray imaging for the **TPPOMnBr$_2$**-based film scintillator. X-ray images of a metallic spring in the capsule (b) and circuit board (c) based on the **TPPOMnBr$_2$**-based film scintillator. (d) MTF curve of the **TPPOMnBr$_2$**-based film scintillator measured by the slanted-edge method.

implying the high spatial resolution of the film scintillator. The X-ray imaging ability of the film scintillator was further demonstrated by X-ray imaging of a metallic spring in the capsule and the circuit board. Owing to the difference in X-ray absorbance between the metals and the plastics, the structures of the spring (Fig. 4b) and the circuit (Fig. 4c) could be clearly shown in the X-ray images, indicating the high-performance in X-ray imaging of the **TPPOMnBr$_2$**-based film scintillator.

In summary, we developed an aromatic moiety-free strategy to tune the excited states of the neutral luminescent manganese(II) halide. The tri(pyrrolidin-1-yl)phosphine oxide (TPPO) was employed as a new ligand to design the manganese(II) complex. The prepared **TPPOMnBr$_2$** not only showed a bright green photoluminescence with short excited state lifetime under UV light, but also exhibited an intense X-ray excited luminescence with a high relative light yield of 10567 photons MeV^{-1}. It should be noted that, owing to the high triplet energy level of the aromatic moiety-free ligand, steric hindrance from the multiple C–H bonds, and the tight molecular packing in the crystals, the dramatic increase of the PLQY of 0.413 is achieved by suppressing the nonradiative deactivation process, which is much higher than that of most of the traditional monodentate ligand-based manganese(II) complexes. Finally, **TPPOMnBr$_2$** was further used as a film scintillator by a solution processed method to demonstrate the application in X-ray imaging with a high spatial resolution value of 11.3 lp mm^{-1} and low detection limit of 34.95 nGy s^{-1}, suggesting its great potential for high-performance X-ray detection. This molecular design strategy will provide valuable guidance in developing highly efficient neutral manganese(II) emitters for low-cost, eco-friendly, and stable X-ray scintillators.

We acknowledge financial support from the National Natural Science Foundation of China (61905120, 62205277, 52073242), National Funds for Distinguished Young Scientists (61825503), Natural Science Foundation of Jiangsu Province of China (BK20190740), China Postdoctoral Science Foundation Funded Project (2018M640506), Start-up Fund for RAPs under the Strategic Hiring Scheme (P0035922), the Hong Kong Research Grants Council (PolyU 15305320), CAS-Croucher Funding Scheme for Joint Laboratories (ZH4A), and Miss Clarea Au for the Endowed Professorship in Energy (847S). We also gratefully acknowledge the support from the University Research Facility on Chemical and Environmental Analysis (UCEA) of The Hong Kong Polytechnic University.

Conflicts of interest

There are no conflicts to declare.

Notes and references

1 (*a*) Z. Hong, Z. Chen, Q. Chen and H. Yang, *Acc. Chem. Res.*, 2023, **56**, 37; (*b*) Q. Chen, J. Wu, X. Ou, B. Huang, J. Almutlaq, A. A. Zhumekenov, X. Guan, S. Han, L. Liang, Z. Yi, J. Li, X. Xie, Y. Wang, Y. Li, D. Fan, D. B. L. Teh, A. H. All, O. F. Mohammed, O. M. Bakr, T. Wu, M. Bettinelli, H. Yang, W. Huang and X. Liu, *Nature*, 2018, **561**, 88.

2 (*a*) X. Ou, X. Chen, X. Xu, L. Xie, X. Chen, Z. Hong, H. Bai, X. Liu, Q. Chen, L. Li and H. Yang, *Research*, 2021, **2021**, 9892152; (*b*) H. Hatcher, *Nat. Rev. Chem.*, 2022, **6**, 840.

3 (*a*) Q. Ma, Y. Cao, X. Ge, Z. Zhang, S. Gao and J. Song, *Laser Photonics Rev.*, 2024, **18**, 2300565; (*b*) W. Chen, M. Zhou, Y. Liu, X. Yu, C. Pi, Z. Yang, H. Zhang, Z. Liu, T. Wang, J. Qiu, S. F. Yu, Y. M. Yang and X. Xu, *Adv. Funct. Mater.*, 2022, **32**, 2107424.

4 (*a*) J. H. Heo, D. H. Shin, J. K. Park, D. H. Kim, S. J. Lee and S. H. Im, *Adv. Mater.*, 2018, **30**, 1801743; (*b*) B. Yang, L. Yin, G. Niu, J.-H. Yuan, K.-H. Xue, Z. Tan, X.-S. Miao, M. Niu, X. Du, H. Song, E. Lifshitz and J. Tang, *Adv. Mater.*, 2019, **31**, 1904711; (*c*) X. Zhao, G. Niu, J. Zhu, B. Yang, J.-H. Yuan, S. Li, W. Gao, Q. Hu, L. Yin, K.-H. Xue, E. Lifshitz, X. Miao and J. Tang, *J. Phys. Chem. Lett.*, 2020, **11**, 1873; (*d*) X. Chen, M. Li, L. Ge, S. Liu, W. Lv, Y. Yu, Y. Tang, C. Han, M. Li, Y. Tao, L. Xu and R. Chen, *Inorg. Chem.*, 2023, **62**, 16538; (*e*) H. Chen, J. Chen, M. Li, M. You, Q. Chen, M. Lin and H. Yang, *Sci. China: Chem.*, 2022, **65**, 2338.

5 (*a*) W. Ma, Y. Su, Q. Zhang, C. Deng, L. Pasquali, W. Zhu, Y. Tian, P. Ran, Z. Chen, G. Yang, G. Liang, T. Liu, H. Zhu, P. Huang, H. Zhong, K. Wang, S. Peng, J. Xia, H. Liu, X. Liu and Y. M. Yang, *Nat. Mater.*, 2022, **21**, 210; (*b*) J.-X. Wang, L. Gutiérrez-Arzaluz, X. Wang, T. He, Y. Zhang, M. Eddaoudi, O. M. Bakr and O. F. Mohammed, *Nat. Photonics*, 2022, **16**, 869; (*c*) X. Ou, X. Qin, B. Huang, J. Zan, Q. Wu, Z. Hong, L. Xie, H. Bian, Z. Yi, X. Chen, Y. Wu, X. Song, J. Li, Q. Chen, H. Yang and X. Liu, *Nature*, 2021, **590**, 410.

6 (*a*) H. Wang, C. Peng, M. Chen, Y. Xiao, T. Zhang, X. Liu, Q. Chen, T. Yu and W. Huang, *Angew. Chem., Int. Ed.*, 2024, **63**, e202316190; (*b*) J.-X. Wang, I. Dutta, J. Yin, T. He, L. Gutiérrez-Arzaluz, O. M. Bakr, M. Eddaoudi, K.-W. Huang and O. F. Mohammed, *Matter*, 2023, **6**, 217; (*c*) M. Chen, L. Sun, X. Ou, H. Yang, X. Liu, H. Dong, W. Hu and X. Duan, *Adv. Mater.*, 2021, **33**, 2104749.

7 S. Ji, Y. Liu, Y. Wang, H. Zhao, Q. Wang, Q. Meng, Y. Bai, J. Jiang, Q. Shen and F. Liu, *Cryst. Growth Des.*, 2024, **24**, 2094.

8 (*a*) Y. Wang, M. Li, Z. Chai, Y. Wang and S. Wang, *Angew. Chem., Int. Ed.*, 2023, **62**, e202304638; (*b*) Z. Li, F. Zhou, H. Yao, Z. Ci, Z. Yang and Z. Jin, *Mater. Today*, 2021, **48**, 155; (*c*) S. Shi, H. Yao, D. Chen, Z. Li, Z. Xu and Q. Wang, *Adv. Opt. Mater.*, 2023, **11**, 2300795.

9 (*a*) P. Tao, S.-J. Liu and W.-Y. Wong, *Adv. Opt. Mater.*, 2020, **8**, 2000985; (*b*) L. Xu, X. Lin, Q. He, M. Worku and B. Ma, *Nat. Commun.*, 2020, **11**, 4329; (*c*) T. Jiang, W. Ma, H. Zhang, Y. Tian, G. Lin, W. Xiao, X. Yu, J. Qiu, X. Xu, Y. M. Yang and D. Ju, *Adv. Funct. Mater.*, 2021, **31**, 2009973; (*d*) Z.-L. He, J.-H. Wei, J.-B. Luo, Z.-Z. Zhang, J.-H. Chen, X.-X. Guo and D.-B. Kuang, *Laser Photonics Rev.*, 2024, 2301249; (*e*) Q. Yang, M.-Q. Yu, Z.-A. Su, Z. Pei, D. Peng, G. Peng and X.-M. Ren, *Inorg. Chem.*, 2023, **62**, 5791; (*f*) X.-F. Sun, P.-F. Li, W.-Q. Liao, Z. Wang, J. Gao, H.-Y. Ye and Y. Zhang,

Inorg. Chem., 2017, **56**, 12193; (*g*) P. She, Y. Ma, Y. Qin, M. Xie, F. Li, S. Liu, W. Huang and Q. Zhao, *Matter*, 2019, **1**, 1644.

10 (*a*) G. Hu, B. Xu, A. Wang, Y. Guo, J. Wu, F. Muhammad, W. Meng, C. Wang, S. Sui, Y. Liu, Y. Li, Y. Zhang, Y. Zhou and Z. Deng, *Adv. Funct. Mater.*, 2021, **31**, 2011191; (*b*) S. Yan, W. Tian, H. Chen, K. Tang, T. Lin, G. Zhong, L. Qiu, X. Pan and W. Wang, *Adv. Funct. Mater.*, 2021, **31**, 2100855; (*c*) Z. Zhou, H. Meng, F. Li, T. Jiang, Y. Yang, S. Liu and Q. Zhao, *Inorg. Chem.*, 2023, **62**, 5729; (*d*) L. Mao, J. Chen, P. Vishnoi and A. K. Cheetham, *Acc. Mater. Res.*, 2022, **3**, 439; (*e*) P. She, Z. Zheng, Y. Qin, F. Li, X. Zheng, D. Zhang, Z. Xie, L. Duan and W.-Y. Wong, *Adv. Opt. Mater.*, 2023, 2302132.

11 D. Goodgame and F. A. Cotton, *J. Chem. Soc.*, 1961, 3735.

12 M. Bortoluzzia and J. Castroc, *J. Coord. Chem.*, 2019, **72**, 309.

13 M. Bortoluzzi, J. Castro, F. Enrichi, A. Vomiero, M. Busato and W. Huang, *Inorg. Chem. Commun.*, 2018, **92**, 145.

14 Z. Jin, B. Tu, Y. Li and M. Li, *Acta Crystallogr.*, 2005, **E61**, m2510.

15 Y.-J. Deng, X. Liang, F.-Y. Li, M.-Z. Wang, Z.-J. Zhou, J.-W. Zhao, F. Wang, S.-J. Liu and Q. Zhao, *Laser Photonics Rev.*, 2023, **17**, 2300043.

16 G.-M. Song, M.-Z. Li, S.-Z. Zhang, N.-Z. Wang, P.-F. Gong, Z.-G. Xia and Z.-S. Lin, *Adv. Funct. Mater.*, 2020, **30**, 2002468.